JOURNAL OF GEOPHYSICAL RESEARCH, VOL. 99, NO. A6, PAGES 11,043–11,062, JUNE 1, 1994

Empirical model of the Io plasma torus: Voyager measurements

Fran Bagenal

Department of Astrophysical, Planetary and Atmospheric Sciences, University of Colorado, Boulder

Abstract. We present a description of plasma conditions in the Io plasma torus, between 5 and 10 R_J, based on Voyager 1 observations obtained in March 1979. The model includes updated analyses of Plasma Science (PLS) data obtained along the spacecraft trajectory as well as Ultraviolet Spectrometer (UVS) observations of composition made remotely from Jupiter. The plasma characteristics observed along the spacecraft trajectory have been extrapolated along magnetic field lines by numerically solving the equations of diffusive equilibrium to produce radial profiles of plasma properties at the centrifugal equator as well as maps of the densities of the major ionic species in a meridian plane. The diffusive equilibrium distribution of plasma along magnetic field lines depends mainly on $T_{||}$. Unfortunately, we only have measurements of $T_\perp$ and must make assumptions about the thermal anisotropy of the plasma. We assume the thermal populations and the suprathermal electrons to be isotropic. The suprathermal ions have probably been recently picked-up and are expected to be highly anisotropic. Varying the thermal anisotropy of the hot ions between A=$T_\perp/T_{||}$=1 to 5 has a minor effect on the plasma maps but makes a significant difference to the fraction of hot ions in the plasma when integrated over a complete shell of magnetic flux. We have found that the vertical extrapolation of plasma density is insensitive to the geometry of different magnetic field models except inside 5 R_J (where the plasma scale height is comparable to uncertainties in the location of the centrifugal equator) and outside 8 R_J (where the magnetospheric current sheet significantly perturbs the magnetic field). The radial profile of flux tube content (NL^2) exhibits the same "precipice", "ledge," and "ramp" features as previous studies as well as confirming small - scale features which indicate local sources of plasma in the cold torus and near the orbit of Europa. The observations of O^{++} and molecular (SO_2^+ or S_2^+) ions inside 5.4 R_J, far from Io, in a region of cold dense plasma, remain difficult to explain, indicating either strong temporal variability in the Io plasma source or a strong source of plasma, possibly from the dissociation of dust, inside Io's orbit. Further evidence of a Europa source are the decrease in the ratio of sulfur to oxygen ions and the increase in plasma temperature outside 8 R_J.

Introduction

The toroidal cloud of plasma surrounding the orbit of Io was first detected from ground-based observations of optical line emissions from S^+ ions [*Kupo et al.*, 1976]. The Voyager 1 flyby of Jupiter in 1979 provided detailed measurements of the Io plasma torus both from the strong emissions in the EUV, observed remotely by the Voyager Ultraviolet Spectrometer (UVS) [*Broadfoot et al.*, 1979], as well as in situ measurements made by the the Plasma Science (PLS) instrument [*Bridge et al.*, 1979]. Each of these techniques for measuring the plasma properties in the torus has its pros and cons. The remote sensing techniques provide good temporal and spatial coverage but suffer from being integral measurements along the line of sight as well as being dependent on accurate atomic data and calibration of the instrument for interpretation of the spectra. The in situ observations provide detailed measurements of the velocity distribution but suffer from limited spatial and temporal coverage as well as poor determination of parameters for individual ionic species in the warm region of the torus where the spectral peaks for different species overlap. Since these two data sets are complementary, there is considerable benefit in combining them to construct a better description of the plasma conditions in the torus. The UVS scans of the torus show that, to first order, the torus is longitudinally symmetric, with the strongest gradients in the vertical and radial directions.

Paper number 93JA02908.
0148-0227/94/93JA-02908$05.00

The first two-dimensional (2D) model of the torus was given by [*Bagenal et al.*,1980], who used the ion temperature determinations from inbound Vogager 1 measurements with a simple expression for an exponential scale height distribution and extrapolated the in situ ion density measurements along dipolar magnetic field lines. A little later, *Bagenal and Sullivian* [1981] replaced the exponential scale height distribution by a diffusive equilibrium density distribution along magnetic field lines in Io torus. They assumed that the plasma would diffuse along magnetic field lines under centrifugal, gravitational, pressure gradient and ambipolar electrostatic forces until a steady state was reached. They solved the equilibrium distribution for each plasma species in a meridian plane numerically.

Bagenal and Sullivan [1981] used the high-Mach number approximation for the response of the PLS detector to estimate the local electron density, ion composition and temperature along the spacecraft trajectory. These local measurements were extrapolated along dipolar magnetic field lines, under the assumption of longitudinal symmetry, to produce a 2D map of electron density in a meridian plane. This original map of the torus was incorporated by *Divine and Garrett* [1983] in an empirical description of the plasma environment of the Jovian magnetosphere necessary for designing the Galileo mission.

Bagenal et al. [1985] reported a factor of 2 error in the ion temperatures published by *Bagenal and Sullivan*, [1981]. They recalculated the 2D density map with the higher temperatures, producing a torus that was more extended latitudinally ($\sqrt{2}$ increase in scale height to first order).

Since 1985, we have reanalyzed the PLS data using the full response of the detectors to low Mach number plasma flows. This has allowed better determination of the electron density and temperature [*Sittler and Strobel*,1987] and the ion temperature [*Bagenal*, 1989]. While the ion composition is well determined in the inner torus region (<5.7 R_J) where the plasma is cold [*Bagenal* 1985], the ion composition is poorly determined from PLS measurements between 5.7 and 11 R_J.

In this paper we report on a new model of the plasma torus based on the PLS measurements of electron density, electron temperature [*Sittler and Strobel*, 1987] and ion temperature [*Bagenal*, 1989] plus the Voyager UVS determination of ion composition (D. E. Shemansky, personal communication, 1991) [*Bagenal et al.*, 1992].

As before, the plasma conditions are extrapolated from the spacecraft location (close to the centrifugal equator) along magnetic field lines under the assumption of diffusive equilibrium. We start with a description of the extrapolation technique which involves numerical solution of 13 simultaneous equations. In a later paper, (Y. Mei, R. M. Thorne and F. Bagenal, "Analytical model for the density distribution in the Io plasma torus", submitted *Journal of Geophysical Research*, 1994, hereafter referred to as Paper 2) we give an analytical approximation that is valid for regions where the electrons are colder than the ions.

After describing the data used in the model, we discuss the radial profiles of plasma density at the centrifugal equator. These equatorial densities have then been extrapolated over a grid in the meridian plane to make 2D maps of electron and plasma density. Finally, we discuss how we have integrated the plasma density over a flux tube to derive profiles of the total flux tube content and composition.

Model

Method

The method for calculating the spatial distribution of plasma in the torus is similar to that used before by *Bagenal and Sullivan* [1981] (following work by *Angerami and Thomas* [1964], on the Earth's magnetosphere) and as discussed in more detail in Paper 2. The plasma is assumed to be in diffusive equilibrium so that the spatial distribution in the direction of the magnetic field can be described by parallel force balance. With a single spacecraft passage through the torus it is not possible to separate radial and longitudinal variations. While longitudinal variations have been observed [e.g.,*Morgan*, 1985; *Dessler and Sandel*, 1992], we assume that the variations observed along the spacecraft trajectory are due to radial structure. We hope that this numerical model of a longitudinally-symmetric torus will be a useful reference for future studies of longitudinal, as well as temporal variations.

Under the conditions of diffusive equilibrium, the density (n_α) of each species (with mass m_α, charge q_α and parallel $T_{\alpha\|}$ and perpendicular $T_{\alpha\perp}$ temperatures) can be written as a function of distance along the field s,

$$n_\alpha(s) = n_\alpha(s_0)\exp\left[\sum_j \Phi_j\right] \tag{1}$$

where

$$\sum_j \Phi_j = (1 - \frac{T_{\alpha\perp}}{T_{\alpha\|}}) \log(\frac{B}{B_0}) \tag{2}$$

$$+\frac{1}{2}\frac{m_\alpha}{T_{\alpha\|}}\Omega_J^2(\rho^2 - \rho_0^2) - \frac{q_\alpha}{T_{\alpha\|}}\Phi_E$$

(for derivation of this equation see Paper 2). Each potential Φ_j is referenced to the centrifugal equator (at s_0), where the distance from Jupiter's rotation axis, ρ, has the maximum value for the magnetic field line. The electrostatic potential Φ_E is assumed to be zero at the centrifugal equator. B is the local magnetic field strength and Ω_J is the rotation rate of Jupiter. Equation (1) is solved numerically for N species under the constraint of local charge neutrality, $\sum_\alpha n_\alpha q_\alpha = 0$, determining n_α and Φ_E. A total of 13 species is included in the model: thermal populations of e^-, S^+, S^{++}, S^{+++}, O^+, O^{++}, H^+, Na^+, SO_2^+ as well as suprathermal populations of e_h^-, S_h^+, S_h^{++}, and O_h^+.

Unfortunately, there are no direct measurements of $T_{\|}$. Both ground-based spectroscopic observations and the Voyager PLS instruments essentially measure $T_{\alpha\perp}$. Thus we must make assumptions about the temperature anisotropy of each species ($A_\alpha = T_{\alpha\perp}/T_{\alpha\|}$). For conditions in the torus, isotropization by collisions is very rapid for cold electrons (τ^e ~5 min at 5 eV), slower for hot electrons (τ^e ~2 days at 400 eV) and very slow for ions (τ^i ~50 days at 60 eV [see *Book*, 1986, p. 33]). These time scales should be compared with estimates for radial transport that vary between 1-10 days [*Richardson and Siscoe*, 1981] and 80-150 days [*Shemansky*, 1988]. It is clearly reasonable to assume that the thermal electrons are isotropic. *Sittler and Strobel* [1987] argue that variations in the pressure of hot electrons measured at different latitudes on the inbound and outbound legs of the Voyager 1 trajectory through the torus imply that the suprathermal electrons are highly anisotropic ($T_\perp \gg T_{\|}$). Since inbound/outbound differences could be due to longitudinal variations and our model is not very sensitive to the hot electron anisotropy, we have assumed $T_\perp = T_{\|}$ for the suprathermal electrons. For the ions, *Smith and Strobel* [1985] calculated the velocity diffusion due to collisions between ions that start as pick up ions and found that the perpendicular velocity distribution of each ion species developed a quasi-thermal core with a nonthermal high-energy tail unless the life time in the torus was less than ~6 days. *Smith and Strobel* [1985] ignored the velocity distribution parallel to the field, arguing that pitch angle scattering due to wave-particle interactions is a small effect. The tilt of the magnetic dipole introduces a finite initial velocity parallel to the field so that $T_{\|\text{pickup}}$=7.5, 15 eV for O^+, S^+ ions [*Siscoe*, 1977]. Relaxation of such ions due to collisions with a background plasma of, say, $T_{\|}$=60 eV occurs quite rapidly ($\tau^i_{\|}$ ~few hours [see *Book*, 1986, p. 32]). The problem is that we do not know $T_{\|}$ for even the bulk of the ions. For our model, the thermal populations are assumed to have isotropic velocity distributions with $T_{\alpha\perp} = T_{\alpha\|}$ (so that the first, magnetic mirror term in equation (2) is zero). We have investigated the effects on the model of these suprathermal ions having a thermal anisotropy $A = T_{\alpha\perp}/T_{\alpha\|}$ equal to 1-5.

To solve the set of equations (1), we require the density and temperature of all species plus the anisotropy of the hot ions at a set of reference points S_o. We have started with the plasma measurements taken by the Voyager 1 PLS instrument during the inbound passage through the torus, from 10 to 5 R_J, between 0400 and 1100 on March 6, 1979. During this period the Voyager 1 spacecraft remained close to Jupiter's equatorial plane (ascending from -1.2 to 5.8° System III latitude) with changes in System III longitude from 50 to 240° (due mainly to Jupiter's rotation). Because of the 9.6° tilt of Jupiter's dipole axis with respect to the planet's rotation axis, the spacecraft's centrifugal latitude oscillated by approximately 2/3x9.6 = 6.4° with a 10-hour period. As the spacecraft traversed the torus the centrifugal latitude rose from −7° at 10 R_J to a maximum of 1.4° at 6 R_J and then decreased to −2° at 4.9 R_J.

The PLS instrument is a set of modulated-grid Faraday cups which measure fluxes of ions and electrons in the energy-per-charge range of 10 to 5950 V (described by *Bridge et al.*, [1977]. The PLS electron measurements in the torus are described by *Sittler and Strobel* [1987]. Estimates of density and temperature of the thermal "core" and the suprathermal "halo" electron populations were obtained throughout the magnetosphere except in the inner region of the torus (<5.7 R_J), where the energy of the bulk of the electrons fell below the 10 eV threshold of the instrument. The values used in this paper are from fitting the low energy part of the electron spectrum with Maxwellian distributions [*Sittler and Strobel*, 1987]. For examples of electron spectra in the torus, see *Belcher* [1983]. The temperatures of the suprathermal population shown in Figure 5 of *Sittler and Strobel* [1987], derived from moment integration of the whole electron spectrum, are rather higher. While the contribution of the suprathermal electrons is not important for the latitudinal distribution of plasma, we point out that they can be critical for estimates of emission intensities and ionization rates. To measure the properties of the ions, the PLS ion detectors need to be directed towards the plasma flow and hence ion measurements were only possible on the inbound passage through the torus, when the detectors faced the corotation direction. Analysis of the measured ion energy-per-charge spectra obtained in the plasma torus is complicated by several factors: (1) the large number of ionic species known to be present, including two dominant ions, S^{++} and O^+, which share the same mass/charge ratio, and cannot be separated by an energy/charge detector; (2) the instrument was optimized for measuring the supersonic flow of the solar wind and has a complex response to transsonic flows that are found in some regions of the torus; (3) when the plasma is warm, the spectral peaks of different ionic species overlap. These difficulties in determining the ion properties in the torus are discussed by *Bagenal and Sullivan* [1981] (but see correction in *Bagenal et al.*, [1985] and *Bagenal* [1989]). When the plasma is supersonic, as in the cold region of the torus inside 5.6 R_J, the ion properties (density, temperature, and flow velocity of each species) are well determined from the spectra [*Bagenal*, 1985, 1989].

Unable to resolve the difficulties in determining the plasma composition from the PLS data in the warm region of the torus, we have turned to remote observations of EUV emissions from the torus obtained by the UVS instrument [*Broadfoot et al*, 1979] a few days before Voyager 1 passed through the torus. As Voyager 1 approached Jupiter, the UVS instrument scanned east-west across the torus obtaining spectra of emissions between 550 and 1200 Å. Shemansky (D.E. Shemansky, personal communication, 1991) derived the plasma composition at 0.5 R_J radial intervals between 5.75 and 8.25 R_J by averaging and fitting spectra from these scans [*Bagenal et al.*, 1992]. The sources and accuracy of data for the torus model are summarized in Table 1.

Table 1. Input to Plasma Torus Model

Component	Quantity	Location, R_J	Accuracy, %	Data Source	Reference
Thermal electrons	n_e, T_e	>5.7	10-15	PLS electron detector	S&S
		<5.7	n_e~10	PLS ion detector, assuming	B
			T_e~20	$n_e = \Sigma n_i Z_i$ and T_e=T_i	
Halo electrons	n_{eh}, T_{eh}	>5.7	~50	PLS electron detector	S&S
Thermal ions	n_i/n_e	<5.7	~10	PLS ion detector	B
		5.75-8.25	15-40*	UVS spectra	DES
		>8.25	~30	PLS ions in plamasheet (>11 R_J)	McN
	T_i	<5.7	10	$T_{\perp i}$ PLS ion spectra,	B
		>5.7	~20	$T_{\parallel i} \equiv T_{\perp i}$	B
Suprathermal ions	n_{ih}/n_e	<5.7	20	PLS ion detector	B
		>5.7	50	PLS ion detector	B
	T_i	<5.7	20	$T_{\perp i}$ PLS ion detector	B
		>5.7	50	$T_{\parallel i} \equiv T_{\perp i}$ / A_i, where A_i=1-10	

S&S, *Sittler and Strobel* [1987]; B, *Bagenal* [1985], *Bagenal* [1989] and this paper; DES D.E. Shermansky (personal communication 1991) and *Bagenal et al.* [1992]; and McN, *McNutt et al.* [1981].

*Uncertainties in the UVS composition increase from about 15% at 5.25 R_j to about 40% at 8.25 R_J.

Input Values

Thermal plasma. Figure 1a shows radial profiles of electron density, measured at the spacecraft. The smooth, model profile (solid line) closely follows the Sittler and Strobel profile (dashed line). A full set of PLS measurements is made every 96 s. For the torus model we have varied the sampling in the radial direction to match major features in the density profile. The electron density in the vicinity of the spacecraft was also derived by *Warwick et al.* [1979] from the frequency of upper hybrid emission observed by the Planetary Radio Astronomy (PRA) instrument (dotted line). The two sets of values agree very closely (<10%) except outside 7.5 R_J, where the 20% difference remains within the uncertainty of the PRA measurements. The three peaks, at 5.9, 5.7, and 5.3 R_J, are features common to all profiles.

In Figure 1, the temperatures of the thermal components of the plasma are plotted. The warm, outer torus is clearly separated from the cold, inner torus by the drop, by a factor of 5, in the ion temperature between 5.7 and 5.6 R_J. The "notch" at 5.6 R_J is real, the localized temperature minimum being evident from the PLS ion spectra (see Figure 2 of *Bagenal* [1985]). Outside 5.7 R_J the electrons are generally about a factor of 10 colder than the ions while inside 5.7 R_J, the electrons are too cold to be measured by the PLS instrument [*Sittler and Strobel*, 1987]. Following *Sittler and Strobel* [1987] we assume that the ion temperature is an upper limit for the electron temperature so we have run the electron profile into the ion temperature profile because the collisional equilibration time is sufficiently short that we expect $T_i = T_e$ inside 5.4 R_J (τ_{ei} ~1 day [see *Book*, 1986, p. 34]. Note that the general increase in temperature of both the ions and electrons >5.7 R_J is contrary to one's expectation that the plasma should cool as it expands on diffusing outwards, away from the source near Io. We shall return to this enigma later. Similarly, the outer part of the electron temperature profile could be interpreted in terms of either an enhanced energy source between 7.5 and 8 R_J or perhaps a loss of electron energy associated with fresh sources of plasma (the pick up process produces cold electrons) near the orbit of Europa at 9.4 R_J.

Suprathermal Plasma. Figure 2 illustrates the properties of the suprathermal populations. Throughout the torus the hot electron population remains less than a few percent of the total electron density and with temperatures of 100-400 eV. For most purposes this population can be completely ignored.

The suprathermal ions, which are about 10 times hotter than the thermal ions form a distinct nonthermal tail to the ion energy spectra [see *Bagenal*, 1989; *Bagenal et al.*, 1992]. The composition of these hot ions is quite unknown and, correspondingly, their temperature and density can only be estimated to 30-50% accuracy. These suprathermal ions form >10% of the ion population outside 5.4 R_J. Inside 5.4 R_J they remain clearly visible in the spectra but drop to a few percent. The enhancement to 20% between 5.6 and 5.4 R_J is curious. This is inside the sharp drop in ion temperature (Figure 1b) and located in the middle of the dip in electron

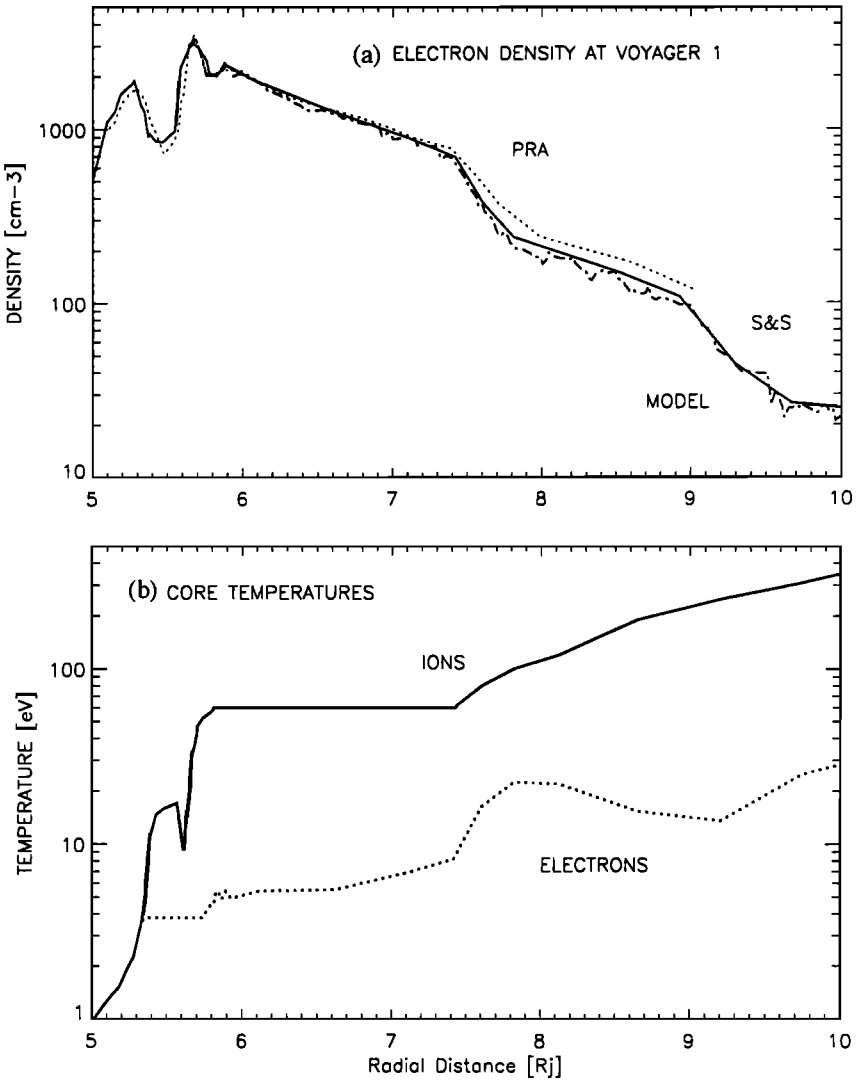

Figure 1. Properties of the thermal plasma components. (a) Electron density measured at the Voyager 1 spacecraft from PRA measurements by *Warwick et al.*, [1979] (dotted line); and from PLS electron measurements by *Sittler and Strobel* [1987] (dashed line). The values used in the current model are shown by a solid line. The x axis is the radial distance from the center of Jupiter to the spacecraft. (b) Temperatures measured at the Voyager 1 spacecraft by the PLS instrument. The x axis is the radial distance to the centrifugal equator of the field line that passed through the spacecraft.

density (Figure 1a). The actual density of hot ions is not enhanced, only the amount relative to the thermal population whose density is depressed in this region.

The obvious source of these suprathermal ions is local pick up. The pick up process produces velocity distributions which are initially highly anisotropic [*Siscoe*, 1977]. In the perpendicular direction the pick up ions form a gyrotropic, mono-energetic beam with the local corotation energy. In the parallel direction there is only a small spread in velocity due to the tilt of the magnetic field. The PLS instrument only measures the dispersion in velocity space in the direction in which the detectors are pointed, more or less perpendicular to the local magnetic field in the magnetosphere. The local pickup energies for O^+ and S^+ ions (dash-dot lines) are shown with the estimated profile of $T_\perp$ for the suprathermal ions (solid line) in Figure 2a. The rough correspondence of these profiles suggests that the suprathermal ions are indeed local pickup ions which have been cooled in the torus (where the density is high) and heated outside (perhaps by mixing with an inwardly diffusing hot population from the middle magnetosphere by the same, as yet unknown, mechanism that heats the plasma in the middle magnetosphere). The parallel temperature of the hot population is completely unknown. For this study we have experimented with anisotropy values between 1 and 10, taking a value of 5 for the standard model.

Magnetic Field Models

Since the centrifugal equator is the plane of symmetry for the vertical distribution of plasma, it is more

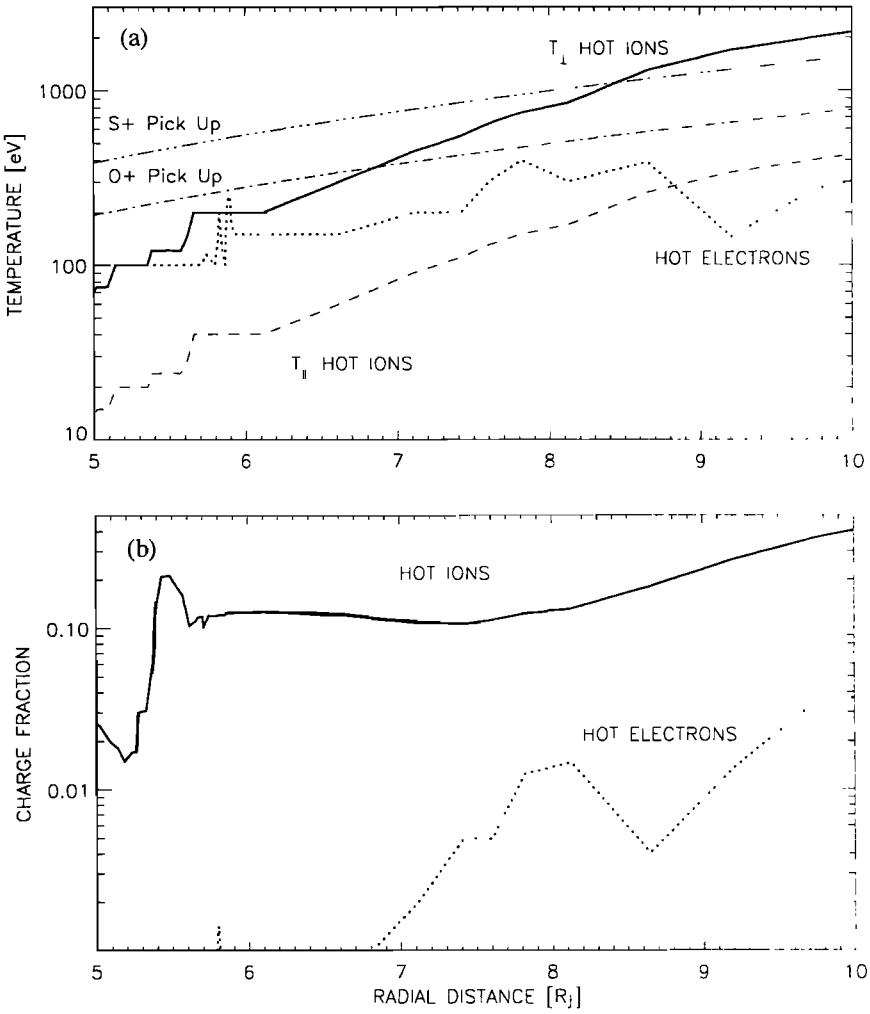

Figure 2. Properties of the suprathermal plasma components. (a) Perpendicular temperatures of the hot ions (solid line) and electrons (dotted line) measured by the PLS instrument. The ions are assumed to have a thermal anisotropy of 5, so that $T_\perp = 5T_\parallel$. The dash-dot lines show the energies of locally picked up O^+ and S^+ ions. (b) the ratio of the density of hot ions and electrons to the total electron density. Both x axes are the radial distance to the centrifugal equator of the field line that passed through the spacecraft.

convenient to have profiles of plasma quantities at the centrifugal equator than at a particular spacecraft location. For the simple geometry of a tilted dipole there is a direct mapping from the spacecraft to the centrifugal equator. To find the equator with more complex field models, we numerically integrate along the field from the spacecraft until we find the location farthest from the rotation axis. At the 5-10 R_J distances of the torus, the non-dipolar contributions to Jupiter's magnetic field are small so that the field lines of the GSFC O4 and O6 models [*Connerney*, 1992] are close to a dipole in shape. The mapping from the spacecraft (at radial distance R_{sc}) to the centrifugal equator (at radial distance R_{cent}) is similar for the different models, as illustrated in Figure 3. In the middle magnetosphere, currents due to drifting energetic particles produce strong perturbations in the magnetic field. Connerney et al. (1982) matched Pioneer and Voyager magnetometer data with an azimuthal current sheet 5 R_J thick, centered on the magnetic equator and extending from 5 to 50 R_J. When the magnetic field due to the current sheet is added to Jupiter's internal field, the net magnetic field in the torus is weaker and field lines are stretched out from a dipole. Figure 3 shows how adding the current sheet has little effect inside 8 R_J (where the spacecraft was close to the equator and where the current sheet is weaker). Outside 8 R_J the radial distance to the centrifugal equator (R_{cent}) is as much as 0.6 R_J greater than R_{sc} in this region, where the spacecraft was well below the equator and the field due to the current sheet becomes significant. The net result of including the current sheet magnetic field in the model is that when the observed plasma densities are extrapolated to the centrifugal equator the radial profile is stretched out (i.e. flattened) beyond 8 R_J.

In addition to the magnetic field geometry, the density extrapolation is obviously very sensitive to how far one is extrapolating the data. The scale height approxi-

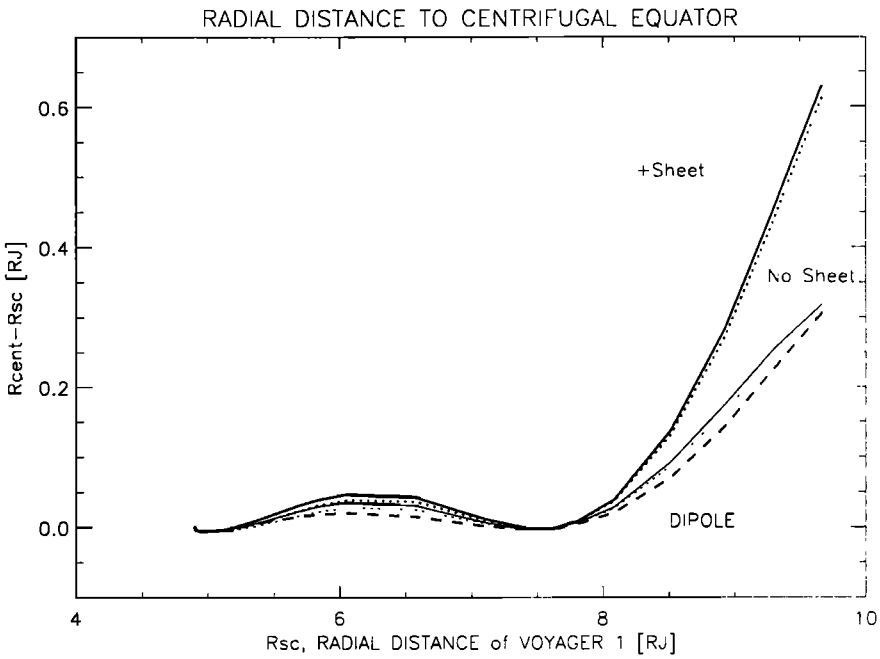

Figure 3. The additional radial distance to the centrifugal equator for field lines that intersected the Voyager 1 spacecraft, calculated using different magnetic field models. The solid (dotted) lines correspond to the O4 (O6) magnetic field models. For the bolder lines the current sheet has been included. The corresponding distance for the offset tilted dipole is given with a dashed line.

mation to the vertical distribution, which is only strictly valid for a single ion species, gives a useful reference. We calculate the scale height for S^+ ions

$$H_i = \left(2kT_i\left(1+Z_iC\right)/3m\Omega_J{}^2\right)^{1/2}$$

$$= 0.64\left(T_i\left(1+Z_iC\right)/A_i\right)^{1/2}$$

where $C = T_e/T_i$, Z_i is the charge state and A_i is the mass number. We have plotted in Figure 4 the vertical distance z, of the spacecraft from the centrifugal equator, relative to the S^+ scale height, H, along the spacecraft trajectory through the torus. Throughout the torus the spacecraft remained less than a scale height away from the centrifugal equator, except inside

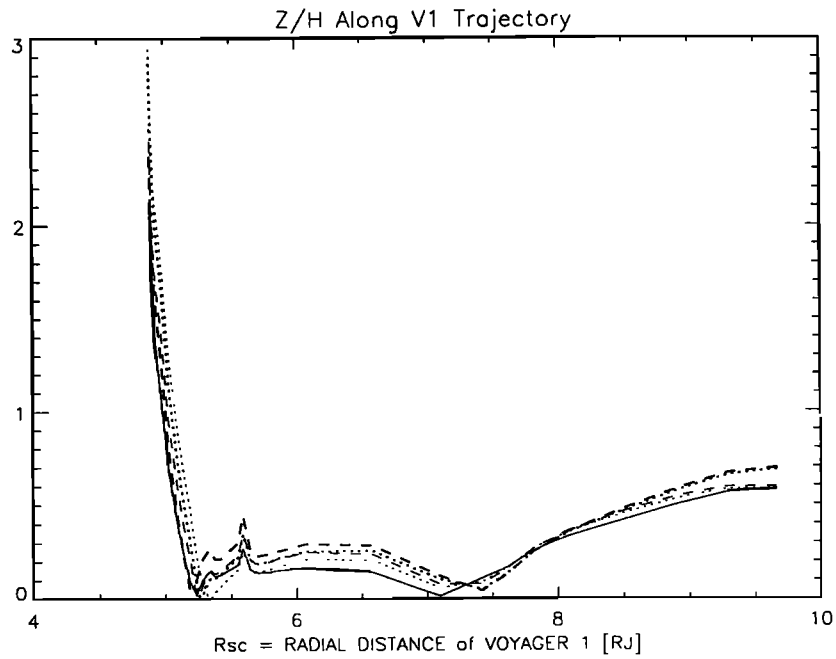

Figure 4. The ratio of the vertical distance of the Voyager 1 spacecraft from the centrifugal equator to the local scale height of S^+ ions. The solid line is for a dipole field. The dashed (dotted) lines correspond to the O4 (O6) magnetic field models. For the bolder lines the current sheet has been included.

5.3 R_J, where the combination of increasing the value of z and decreasing H (due to the dropping ion temperature) results in rapidly increasing z/H. Thus, inside 5 R_J, to extrapolate the spacecraft densities to the equator, not only are we extrapolating over more than a scale height but the value of z varies significantly with magnetic field model. The consequence of this sensitivity to z/H is shown in Figure 5, where we compare the measured density at the spacecraft (s/c) with the extrapolated densities at the centrifugal equator for the O4 and O6 magnetic field models, with and without the current sheet. While Figure 5 illustrates the effect of the current sheet flattening the radial profile beyond 8 R_J, it is the differences between the O4 and O6 models that produces radically different density profiles inside 5.1 R_J.

This sensitivity of the vertical location of the centrifugal equator to the magnetic field geometry in the cold torus is also dramatically illustrated by the ground-based observations of SII emissions which show the cold torus to be distinctly "warped". In the long run, measurements of the warp will provide constraints for magnetic field models. For this study, we have restricted the model to radial distances greater than 5.0 R_J because of the strong dependence on magnetic field geometry farther in. The high and inwardly rising densities predicted by the O6 model are probably unrealistic. As a working compromise, we have used the O4 plus current sheet magnetic field model as the standard for this paper.

Plasma Conditions at the Centrifugal Equator

Major Ion Composition

Using the O4 magnetic field with current sheet [*Connerney et al.*, 1982; *Connerney*, 1992], we have extrapolated the plasma conditions at the spacecraft (summarized in Table 1 and Figures 1 and 2) to the centrifugal equator. The resulting density profiles for the electrons and the major ion species are given in Figure 6. It is perhaps easier to obtain a sense of the composition of the torus by examining charge fractions for these species and various ratios (Figure 7).

Inside 5.6 R_J the ionic composition is well-determined by the PLS experiment so that the model profiles are close to those published by Bagenal (1985). Small differences are due to the more recent analysis incorporating a more detailed description of the response of the detector and including suprathermal ions (for example, see the fit to a spectrum in Figure 1 of *Bagenal et al.*, [1992]. Composition is dominated by S^+ and O^+ ions in this cold region of the inner torus. The few percent of O^{++} ions are clearly evident in the spectrum. The very existence of as much doubly ionized material in such a cold plasma, let alone the enhancement between 5.3 and 5.0 R_J, remains an important unresolved issue. Composition of the warm torus plasma, derived by D.E. Shemansky from the UVS emission spectra at 5.75 R_J and beyond, is radically different. O^+ dominates at 40% of the charge fraction, followed by S^{++} at 17% and about 10% S^+. This composition is similar to that derived for the warm torus from observations of UV emissions made by the International Ultraviolet Explorer [*Moos et al.*, 1985], the Hopkins Ultraviolet Telescope [*Moos et al.*, 1991] and the Hubble Space Telescope [*McGrath et al.*, 1993]. We have taken D.E. Shemansky's (model) value of 1.3% for the mixing ratio of O^{++} in the warm torus which is consistent with the HUT detection [*Moos et al.*, 1991] but lower than *Thomas'* [1993] recent measurement of $[O^{++}]/n_e$=3.4%.

As reported by *Bagenal et al.* [1992], at the outer boundary of the torus (7.5 R_J), at the same location as the sharp rise in T_e, the amount of more highly ionized material increases (particularly, O^{++} but also S^{+++}). Overall, there is a dramatic change in the ratio of the total amount of sulfur ions to total oxygen ions (S/O) from a maximum value of 3 in the cold torus at 5.3 R_J to a value of 0.6 in the warm torus, dropping to 0.2 outside. This is hard to explain with the simple idea of SO_2 gas from Io as the sole source of plasma. The enhanced oxygen abundance near the orbit of Europa and the sputtering of water ice as a source of O^+ ions was pointed out by *Bagenal et al.* [1992] and more extensively discussed by *Schreier et al.* [1993]. Similarly, one has to consider the possibility of sulfur being added to, or oxygen being removed from, the cold torus.

Minor Ion Composition

The detection of an ion with a mass/charge ratio of 64 (possibly S_2^+ or SO_2^+) was first reported by *Bagenal and Sullivan* [1981] and discussed extensively by *Bagenal* [1985]. The spectral peak is only visible between 5.35 and 5.1 R_J and corresponds to a density of SO_2^+ or S_2^+ of only 0.5% n_e. There may be more molecular ions farther out than 5.35 R_J but they were not detectable above the background of suprathermal ions. Inside 5.1 R_J the spacecraft was dipping farther below the centrifugal equator, to which the heavy molecular ions are very tightly confined. The problem posed by the detection of molecular ions is how they could have survived without dissociation if they have traveled through the dense region of the torus from Io.

The strong emission from the cloud of neutral sodium atoms that has been observed for the past 20 years suggests that there should also be sodium ions in the torus. There were no clearly identified peaks in the Voyager PLS spectra at mass/charge = 23. Upper limits to the sodium ion abundance could be placed at values <3% to fit the spectrum between the spectral peaks at A/Z=16 and 32.

Finally, there remains the issue of protons. Protons comprise a significant fraction (20-50%) of the plasma in the middle magnetosphere [*McNutt et al.*, 1981]. In the torus, corotating protons have dropped below the 10-eV energy threshold of the PLS detector. Nevertheless, in the cold torus, where the spectral peaks are well resolved, an upper limit of ~0.5% can be placed on the proton density from the part of the distribution

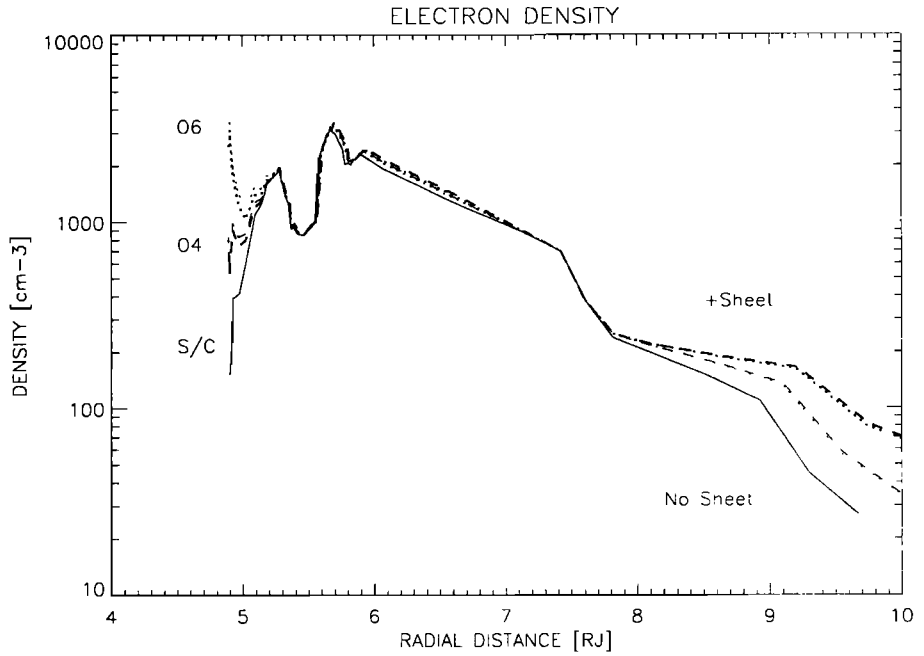

Figure 5. The electron density profile measured at Voyager 1 (solid line) compared with the density at the centrifugal equator for different field models. The solid line is for a dipole field. The dashed (dotted) lines correspond to the O4 (O6) magnetic field models. For the bolder lines the current sheet has been included.

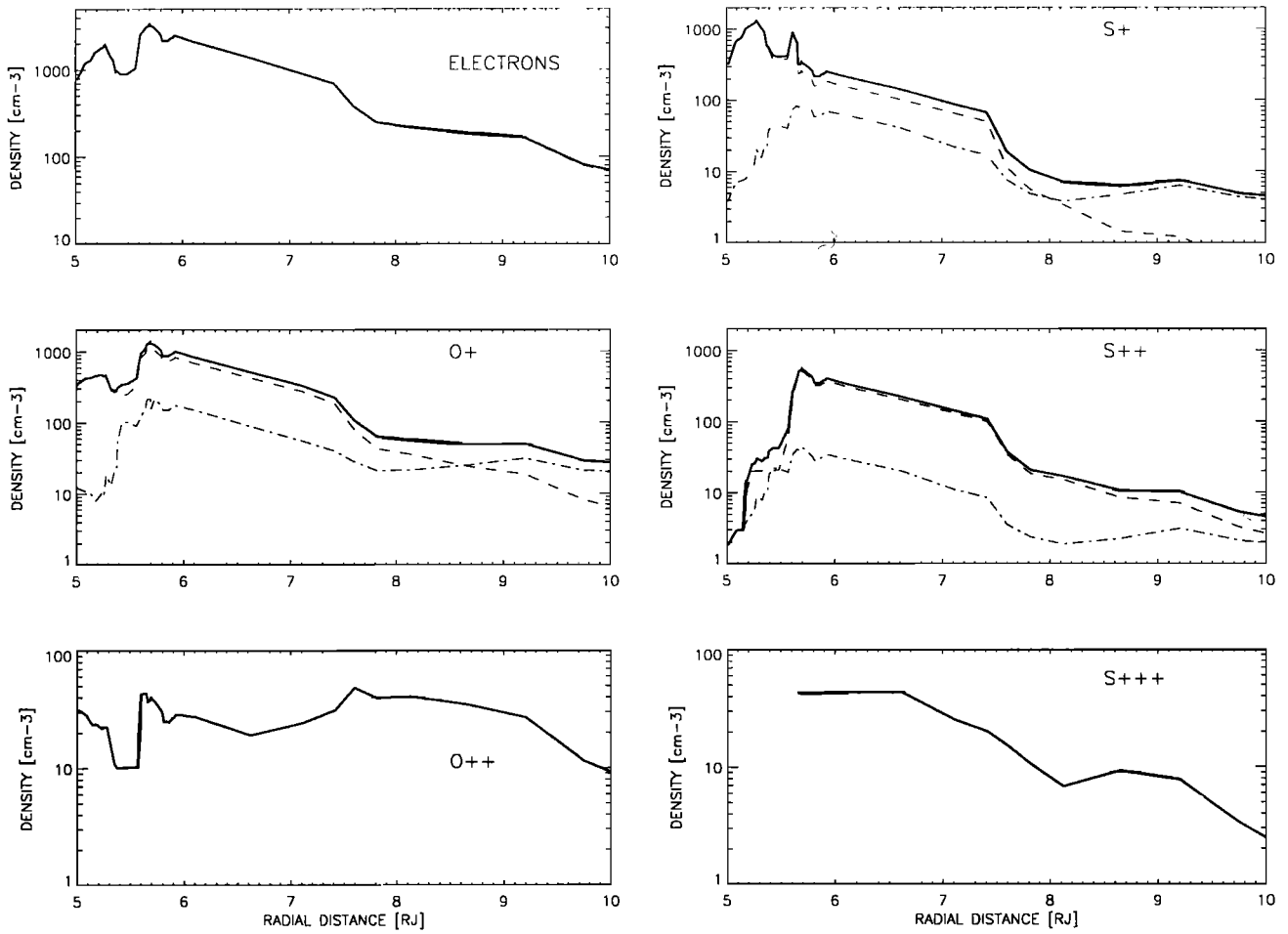

Figure 6. Radial profiles of electron and ion density at the centrifugal equator. The dashed (dash-dotted) lines are for the thermal (suprathermal) populations. The solid lines are the total density for each species.

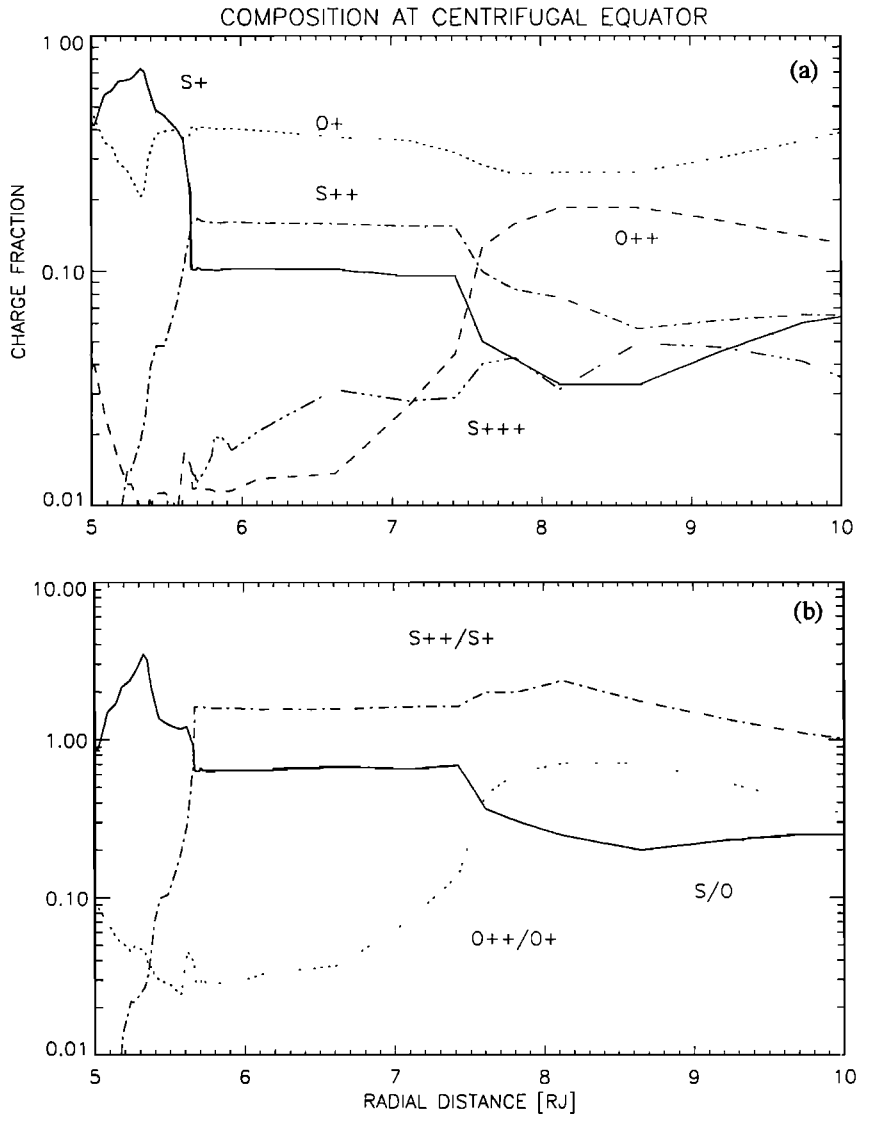

Figure 7. Composition at the centrifugal equator. (a) The ratio of ion density to electron density for the five major ion species. (b) Ratios of ion species. S/O is the ratio $(S^+ + S^{++} + S^{+++})/(O^+ + O^{++})$.

that extends above 10 eV (see spectrum of *Bagenal et al.*, [1992]). *Tokar et al.* [1981] placed limits of 10-15% on the proton density in the warm torus by comparing the dispersion of whistlers that had traveled through the torus with the *Bagenal and Sullivan* [1981] model of the torus. Repeating such a study using the current model would require a reduction in the proton composition. For the current model, we have assumed that protons comprise about 10% of the density in the warm torus.

Two-Dimensional Distribution

While the equatorial profiles were derived using the specific magnetic field geometry along the Voyager 1 trajectory, to generate a 2D model of the plasma distribution in the torus that can be more generally applied we have chosen the geometry of a dipolar magnetic field at System III longitude of 292° (where the magnetic, centrifugal and rotational equators coincide).

Major Species

The equatorial profiles have been extrapolated over a grid to make maps of the densities of the major species in the meridional plane shown in Figure 8. Similar density maps were published by *Bagenal and Sullivan* [1981]. The overall structure remains the same with a vertically-extended warm torus, a cold inner torus and the dense "ribbon" between 5.7 and 5.9 R_J. However, there are significant differences due to the new model (1) correcting the factor of 2 error in T_i by *Bagenal and Sullivan* [1981] [see *Bagenal et al.*, 1985]; (2) using the UVS composition in the warm torus region; (3) including the suprathermal ion population; (4) including the current sheet magnetic field when extrapolating densities from the spacecraft to the centrifugal equa-

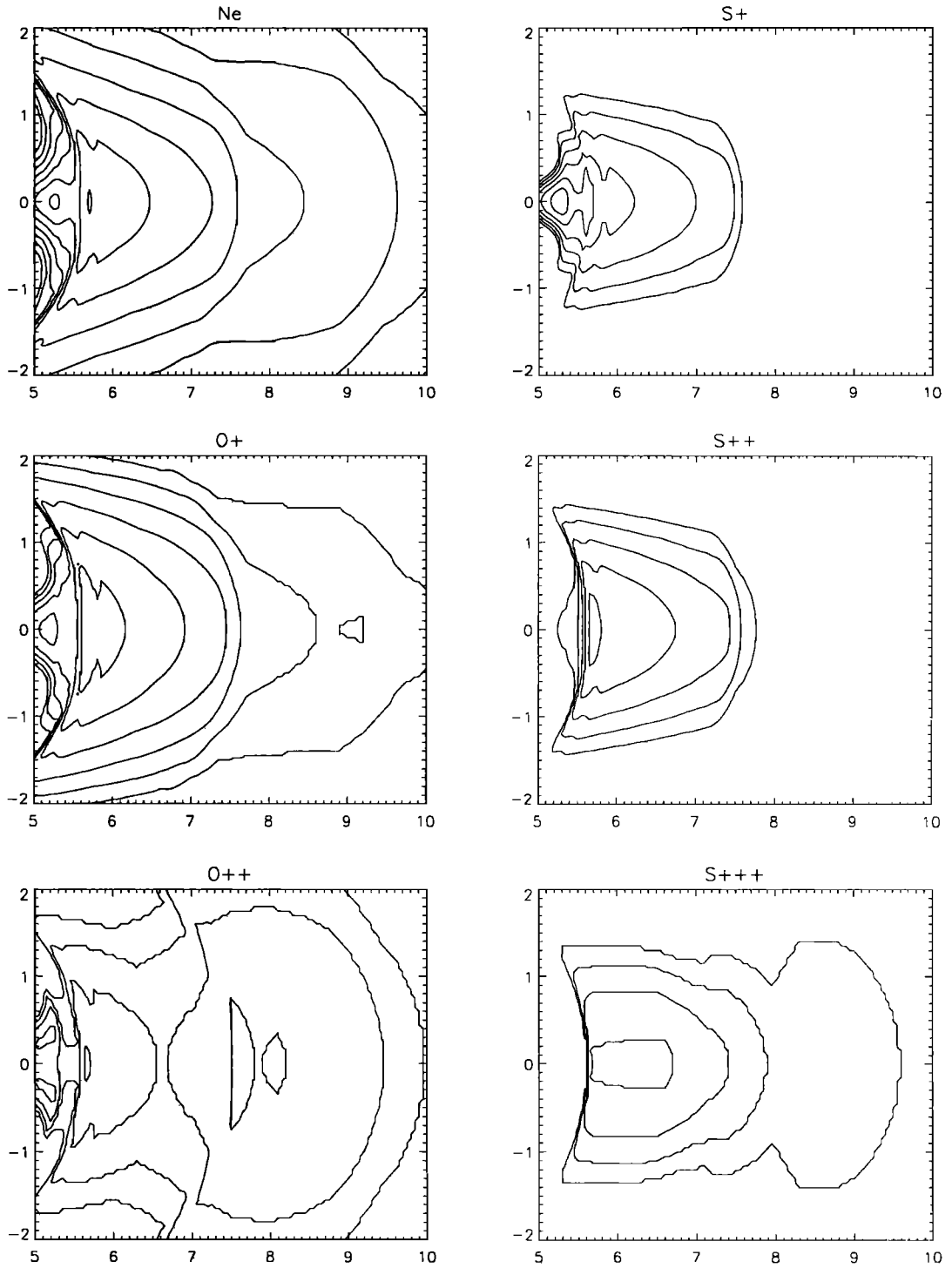

Figure 8. Contours of electron density in the meridian plane for System III longitude of 292°. All contour levels are spaced by factors of 2. For example, the electron contours are 3200, 1600, 800, 400, 200, 100, 50 and 25 cm^{-3}. The contours for O^+, S^+, and S^{++} decrease by factors of 2 from 1600 cm^{-3} and the contours for O^{++} and S^{+++} decrease from 80 cm^{-3}.

tor. The electron density map that has perhaps been used the most extensively to date is the one that was published by *Bagenal et al.* [1985] in which the first of the above problems was addressed. For comparison, we have overlaid the electron densities from the new model on the *Bagenal et al.* [1985] map in Figure 9, using the same contour values. Apart from the effect of using the symmetric field geometry of 292° longitude (rather than the field geometry corresponding to the changing longitude along the spacecraft trajectory) the only significant changes are higher densities extending to higher latitudes in the ribbon region (5.7-5.9 R_J) and

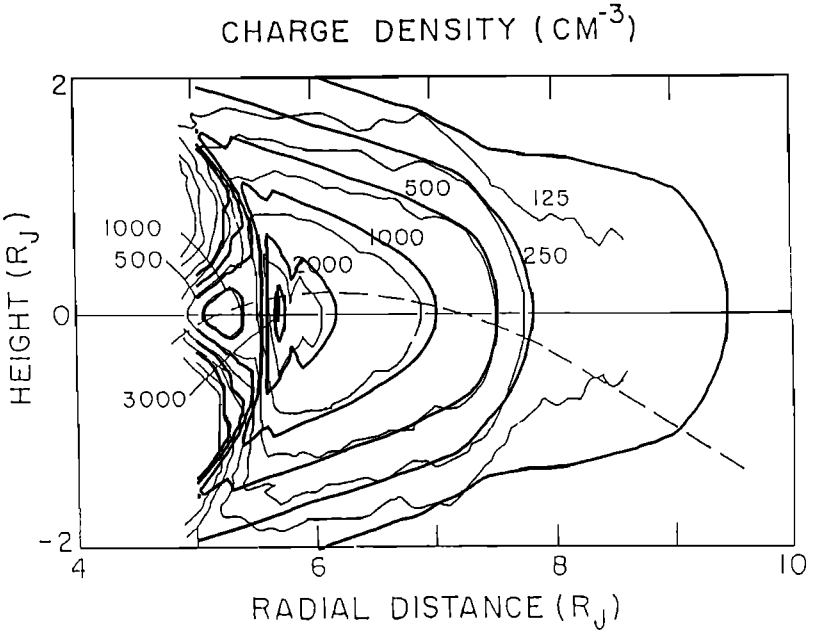

Figure 9. Comparison of the current two-dimensional model of electron density with the previous model of *Bagenal et al.* [1985]. The inbound trajectory of the Voyager 1 spacecraft is given by a dashed line.

higher density at the equator >8 R_J (due to inclusion of the current sheet). It is important to keep in mind the uncertainties in the extrapolation method and the inaccuracies of the measurements when examining these contour maps. While the values are probably accurate to about 10% at the equator, the reliability is probably no better than 50% by ±2 R_J.

Stone et al. [1992] obtained local electron densities from radio emissions detected by the Ulysses space craft when it traversed the Io torus in February 1992. The Ulysses measurements agree with the Voyager model quite well near the equator (8 R_J) but lower densities were measured above and below the equator [*Stone et al.*, 1992]. While such differences might be due to longitudinal or temporal variations, it would be interesting to see if the two data sets can be reconciled by making the "thermal" ions anisoropic ($T_{\|} \ll T_{\perp}$).

For comparison with observations of emissions from the torus, it is more useful to have maps of the product $n_e n_i$ (though one must be cautious because radiation efficiencies of different lines also depend on T_e, which varies considerably between 5 and 10 R_J). Figure 10 shows maps of $n_e n_i/1000$ (using the same contour values as Figure 9). The $n_e n_i$ maps are much more similar for different species than the n_i maps in Figure 8. There is less spread both vertically and radially outwards, especially for O^{++}, O^{+}, S^{+++}, and S^{++}. Note that the $n_e n_i$ maps enhance the "ribbon" feature between 5.7 and 5.9 R_J for all the ionic species and the double maxima of O^{++} density off the centrifugal equator in the cold torus is not present in the $n_e n_i(O^{++})$ map.

Minor Species

Figures 8 and 10 only show the major ionic species. The minor ions (mostly H^{+}) only contribute 10% of the electron density at the equator. Because of its low mass, H^{+} is spread fairly evenly throughout the region and contributes 50% of the density 1.5 R_J above the equator. While the SO_2^{+} and/or S_2^{+} molecular ions comprise only a very small fraction of the plasma, it is interesting, nevertheless, to examine their spatial distribution. Figure 11 is a contour map of the small region in the cold torus where the molecular ions were observed. Outside 5.35 R_J we have left the contours open because the density may be substantial, even though we were not able to detect the molecular ions. Note that these heavy molecular ions are very tightly confined to the equator (H=0.15 R_J at 5.3 R_J) and it would be easy for a spacecraft flying throughout the torus to miss them entirely. In Figure 11 we show the Voyager 1 trajectory as well as the predicted path of the Galileo spacecraft on its inbound passage through the torus when extensive plasma measurements will be made.

Flux Tube Content

For studies of plasma transport in the magnetosphere it is useful to calculate the total number of ions per shell of magnetic flux, N [*Siscoe* 1978]. For dipolar magnetic field geometry, where L is the radial distance of a magnetic field line at the magnetic equator, the relevant quantity is

$$N_i L^2 = 4\pi R_J^3 L^4 \int_0^{\theta_{max}} n_i(\theta) \cos^7\theta \, d\theta$$

which we calculate numerically from the symmetric (292°) plasma model

$$N_i L^2 = 8 \times 10^{28} L^4 \sum_j n_i(\theta) \cos^7\theta \, \Delta\theta_j$$

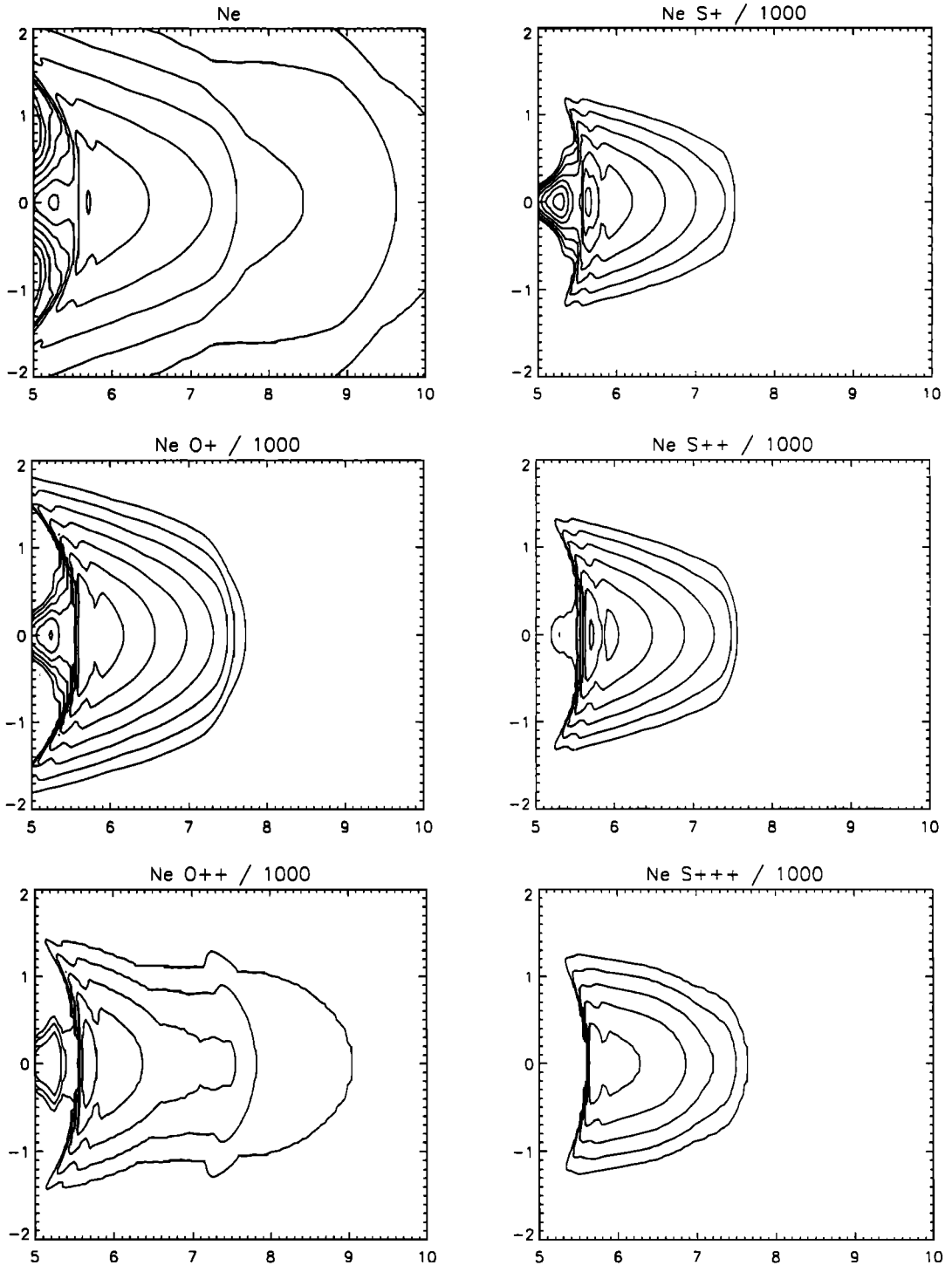

Figure 10. Contours of the product of electron density and ion density (divided by 1000). The geometry and contour levels are the same as in Figure 8.

where the centrifugal latitude, θ, is incremented in steps of $\Delta\theta_j = 0.1°$ to a maximum latitude of 33°. The assumption that the shape of the magnetic field is dipolar is probably quite reasonable throughout the 5-10 R_J region but the volume per unit flux is probably underestimated (by on the order of 20%) beyond 8 R_J, where the current sheet magnetic field becomes significant. We have not taken this effect into account. We have considered, however, the effects of using equatorial density profiles derived from different magnetic field models. Figure 12 shows that the effect of different models is negligible except outside 8 R_J, where the flattened density profiles of the sheet models produces correspondingly enhanced values of the total NL^2.

For comparison with previous profiles we show the NL^2 profile from the standard model (with A=5 and

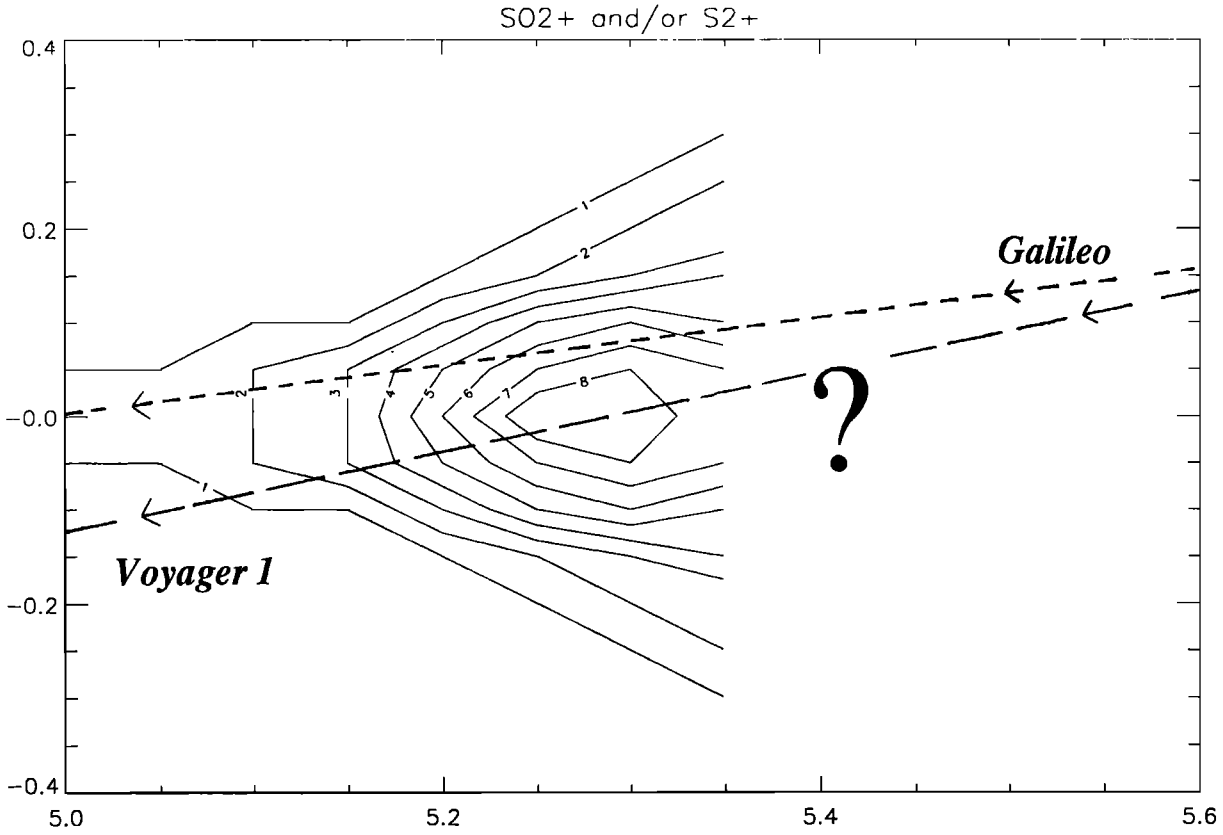

Figure 11. Contours of the density of molecular ions in the cold torus.

the O4+sheet magnetic field) in Figure 13. The smoothed profile used to delineate various dynamic regions by *Siscoe et al.* [1981] has been added (thin line). The new model has made very little difference to the overall shape of the profile; the "precipice" (<5.7 R_J), the "ledge" (5.7 to 7.5 R_J), and the "ramp" regions remain as before. *Siscoe et al.* [1981] propose that if the main source of plasma is confined to near Io's orbit (5.92 R_J) then the steepness of slope in the NL^2 profile corresponded (inversely) to the rate of radial diffusion.

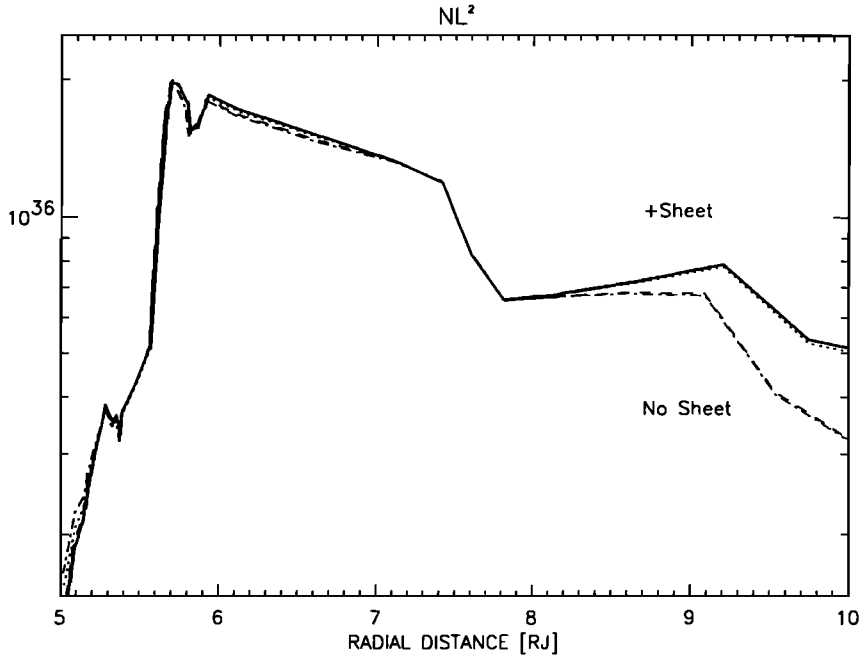

Figure 12. Radial profiles of total flux tube content calculated using different magnetic field models. (A=5 for all cases).

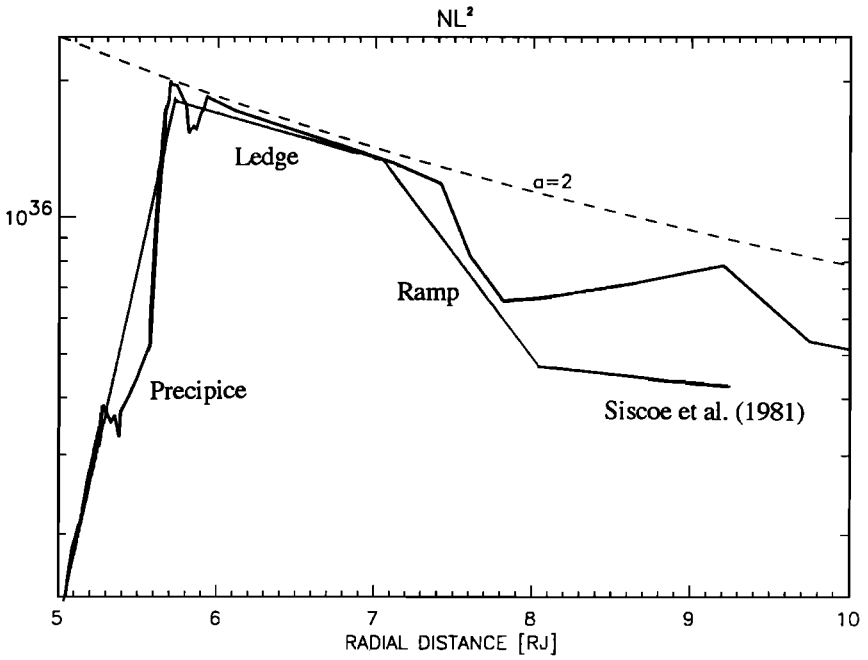

Figure 13. Radial profile of total flux tube content from the current model compared with previous radial profile published by *Siscoe et al.* [1981]. A radial profile of a power law with index a=2 is also shown for comparison.

Thus, the precipice indicates slow inward diffusion in the cold torus (radial transport being inhibited by the centrifugal potential) while the gentle slope of the ledge indicates rapid outward diffusion (enhanced by the centrifugal potential). *Siscoe et al.* [1981] proposed that in the ramp region outward diffusion was inhibited by the outward pressure gradient of energetic (>10 eV) particles that form Jupiter's ring current outside 8 R_J. In the new model the ramp region starts at 7.5 rather than 7 R_J and the enhanced NL^2 farther out supports the idea that Europa (at 9.4 R_J) may be a source of plasma.

In the ledge region of the warm torus the NL^2 profile remains close to a power law with an index of a=2. The NL^2 profile inside 6 R_J is very similar to the published by *Bagenal* [1985]. The maximum value of NL^2 is still at 5.7 R_J, which indicates the source of plasma must be distributed well inwards of Io's orbit (5.92 R_J). *Linker et al.* [1985] have modeled how Io's neutral clouds can

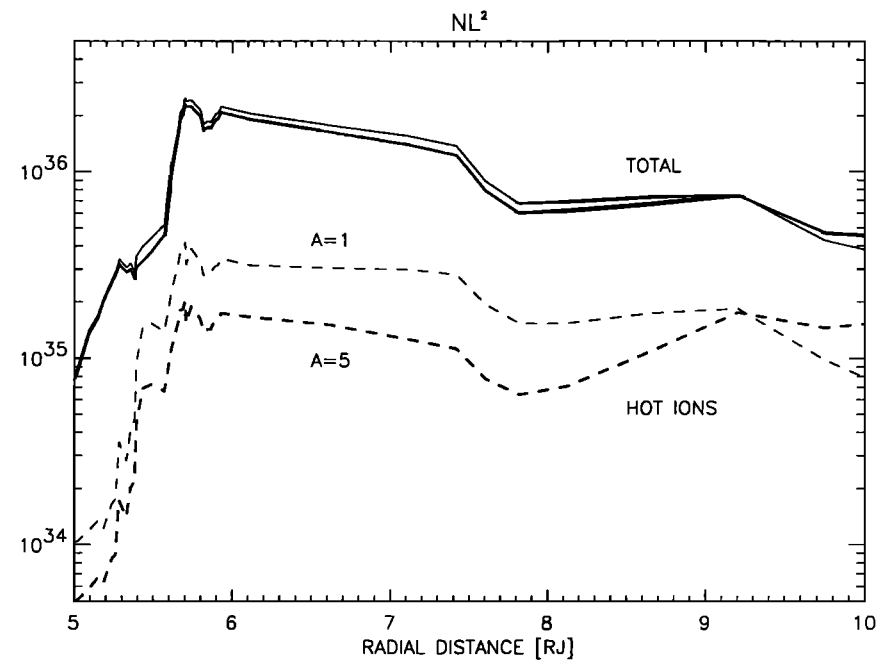

Figure 14. Radial profiles of total flux tube content (solid lines) compared with flux tube content of hot ions (dashed lines) for thermal anisotropies of A=5 (bold) and A=1.

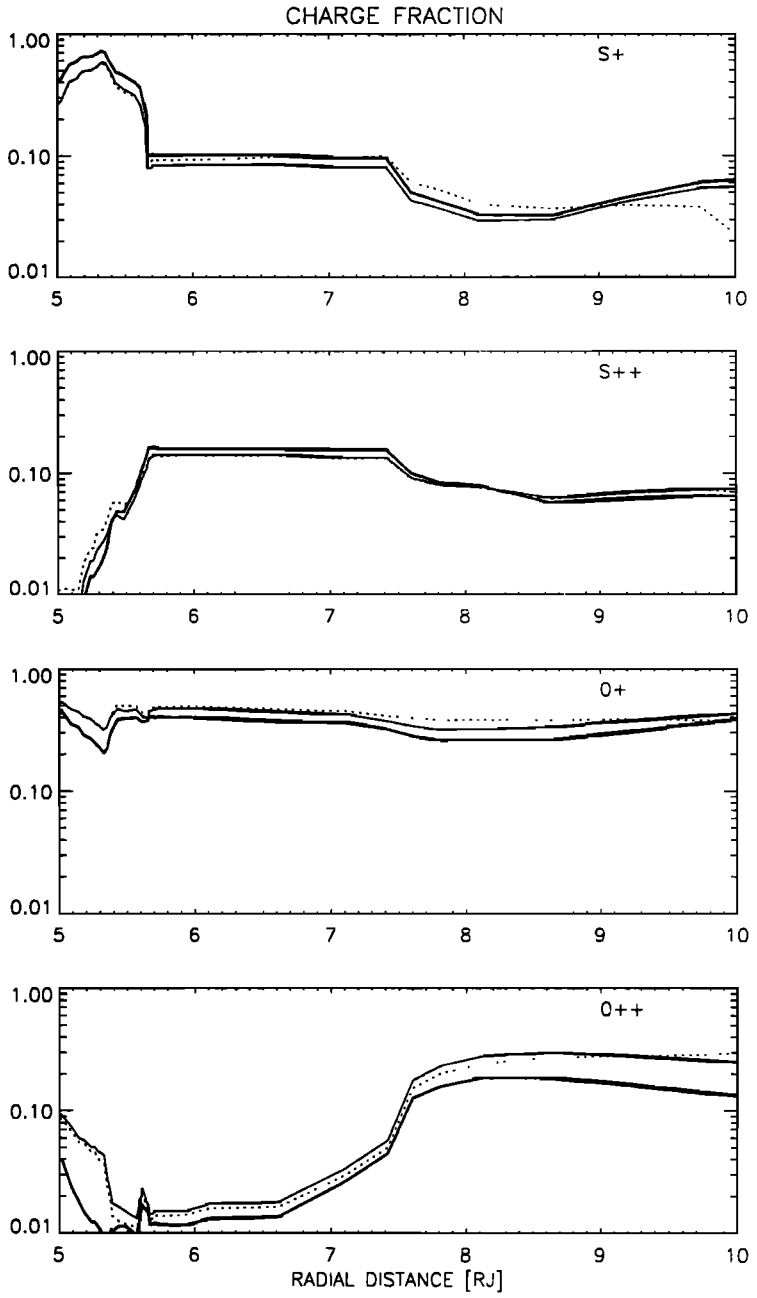

Figure 15. Integrated flux tube charge fractions for A=5 (solid lines) and A=1 (dotted line) compared with equatorial values (bold).

extend inwards to produce a source of plasma in this region. The issue of why there should be a 20% dip at 5.8 R_J, even more distinct in the new model, remains a mystery. Similarly, the change in slope between 5.6 and 5.4 R_J is clearly demonstrated in the new model, perhaps even suggesting a local maximum at 5.3 R_J. This is further evidence that there are local sources of plasma in the cold torus [*Bagenal* 1985].

To illustrate the effect on the NL^2 profile of the suprathermal ion population, we show profiles for difference values of the hot ion thermal anisotropy in Figure 14. Even when A=1, and the hot ions are not confined by the magnetic mirror force, they make a minor contribution to the total flux tube content except between 5.4 and 5.6 R_J and in the outermost region. It should be noted, however, that the NL^2 profile for the hot ions outside 6 R_J is flatter than the total NL^2 profile, suggesting an enhanced source of hot material outside the torus.

Finally, we have compared in Figures 15 and 16 the plasma composition at the centrifugal equator (thick solid lines) with the flux tube-integrated composition for A=5 (thin solid lines) and A=1 (dashed lines). For the thermal population, there is little change when integrated over the flux tube except for O^{++}, which is spread out to high latitudes in the cold torus so that

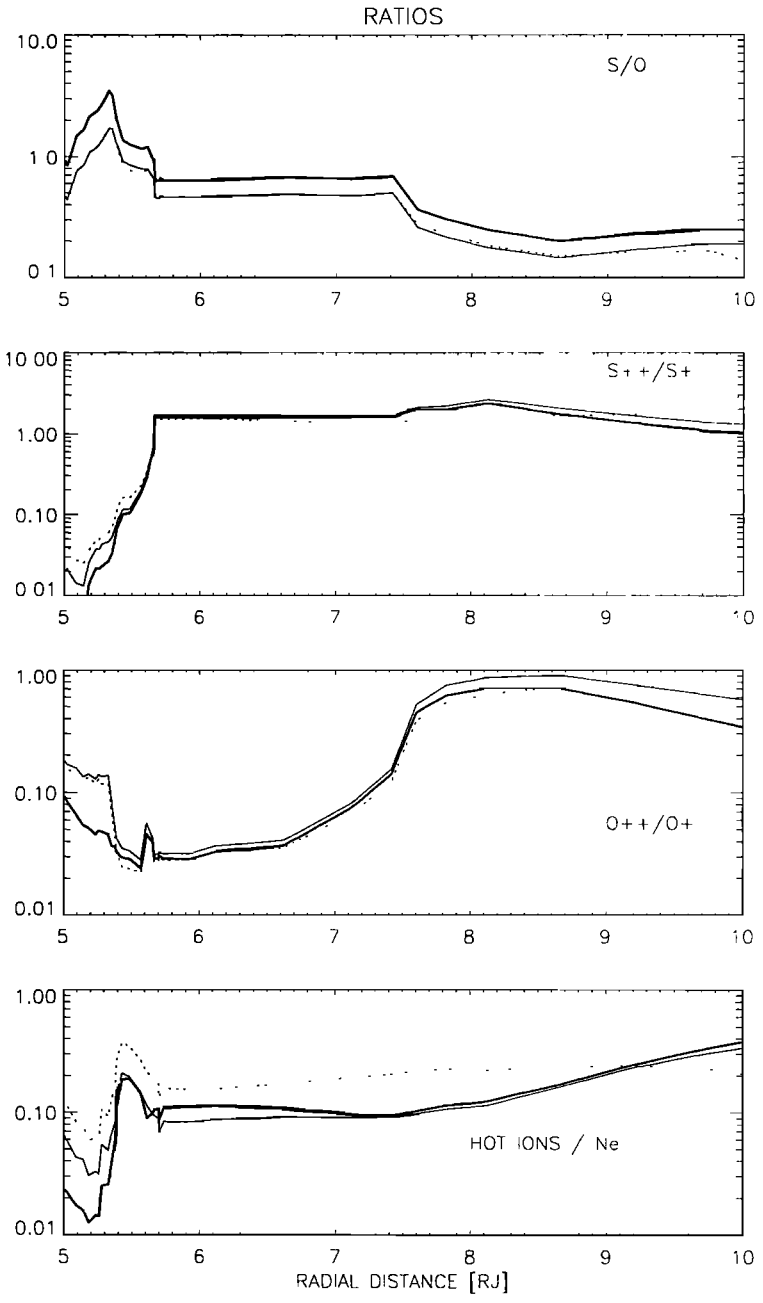

Figure 16. Integrated flux tube composition ratios for A=5 (solid lines) and A=1 (dotted line) compared with equatorial values (bold).

the integrated flux tube charge fraction is increased (to 10%). When considering the composition ratios in Figure 16, it is notable that the flux tube S/O ratio is reduced by 50% over the values at the centrifugal equator due to the lighter oxygen ions being less confined vertically. Integration over the flux tube makes the issue of the presence of O++ in the cold torus much worse, with O^{++}/O^{+} increasing from 10 to 20%.

The bottom panel of Figure 16 illustrates the effect of the thermal anisotropy on the contribution of hot ions to the flux tube content, particularly in the cold torus where making A=1 pushes the hot ion fraction over 30%.

Summary

Model

We have presented a description of plasma conditions in the Io plasma torus, between 5 and 10 R_J, based on Voyager 1 observations. The model includes updated analysis of PLS data obtained along the spacecraft trajectory as well as UVS observations of the plasma composition made remotely while Voyager approached Jupiter. The PLS electron measurements provide the density and temperature of the thermal and suprathermal electrons throughout the region except inside 5.6

R_J where there are few electrons above the 10 eV energy threshold of the instrument. The PLS ion data have been analyzed using the detailed response of the detector to transsonic flow and provide $T_\perp$ for the thermal and suprathermal ion populations throughout the torus. Inside 5.6 R_J and in the middle magnetospheric plasma sheet (>11 R_J) the densities of each ionic species are well determined from the PLS ion measurements. In the warm torus (5.75-8.25 R_J), where the PLS ion instrument cannot distinguish separate ionic species, we have taken the composition determined by D.E. Shemansky from the Voyager 1 UVS measurements (published by *Bagenal et al.*, [1992]). The plasma characteristics observed at the Voyager spacecraft have been extrapolated along magnetic field lines by numerically solving the equations of diffusive equilibrium, producing radial profiles of density, temperature and composition at the centrifugal equator as well as maps of density and composition in the meridian plane. On investigating how the extrapolation is affected by the use of different magnetic field models, we find that the results are not very sensitive to the field model used except inside 5 R_J (where the small scale height of the cold plasma produces a strong sensitivity to accurate determination of the location of the centrifugal equator) and outside 8 R_J (where the magnetic field due to the magnetospheric current sheet becomes significant).

With no direct measurements of $T_\parallel$, we have had to make some assumptions about the thermal anisotropy of each species in order to determine the diffusive equilibrium distribution of density. We have assumed that the thermal ions and electrons are isotropic and that the suprathermal ions have an anisotropy of $A=T_\perp/T_\parallel=1$ to 5.

Results

The resulting 2D maps of density in the torus are similar to those of *Bagenal and Sullivan* [1981] and *Bagenal et al.* [1985]. The major change (illustrated in Figure 9) is that the electron density is distributed farther from the equator in the ribbon region (5.7 to 5.9 R_J) due to the presence of hot ions.

Similarly, the profile of total flux tube content (Figure 13) has not changed radically from *Siscoe et al.* [1981], exhibiting the precipice, ledge, and ramp regions. Smaller features, a 20% dip at 5.8 R_J and a local peak at 5.3 R_J persist. While the large scale features confirm that the main source of plasma must be near Io's orbit with radial transport preferably outwards [*Richardson and Siscoe*,1981], the smaller features are evidence of sources inside the cold torus [*Bagenal*1985] and near the orbit of Europa [*Wu et al.*, 1978; *Intriligator and Miller*, 1982; *Bagenal* 1989; *Schreier et al.*, 1993].

Changing the thermal anisotropy of the hot ions does not change the properties of the torus model very much except that anisotropies as low as $A=T_\perp/T_\parallel=1$ produce high proportions of hot ions when integrated over the whole flux tube (20% overall, increasing to nearly 30% between 5.4 and 5.6 R_J).

The characteristics of regions between 5 and 10 R_J can be summarized as follows:

The inner torus 5-5.4 R_J. The plasma is cold (~1 eV) with few suprathermal ions or electrons. The composition is dominated by S^+ and O^+ with small, but as yet unexplained, quantities of O^{++} and SO_2^+.

The precipice region 5.4-5.6 R_J. There are sharp changes in the slope of NL^2 and in the composition. The suprathermal ions comprise >10% of the density.

The ribbon region 5.6-6 R_J. Here are the highest densities (>3000 cm^{-3}). The temperature and composition are similar to the rest of the warm torus.

The ledge region 6-7.5 R_J. This is the uniform region of the warm torus, where there are gradual changes in density, composition, and temperature.

The ramp region > 7.5 R_J. There is a drop in NL^2, perhaps due to impoundment of the torus material by the middle magnetospheric ring current. The current sheet begins to affect the magnetic field. The ions change in composition towards higher ionization state and higher oxygen fraction. Suprathermal ions are diffusing inwards. Europa is a possible source of plasma in this region.

Issues

The Io plasma torus can no longer be simply described by a single source of plasma near Io's orbit with preferential outward diffusion. There are clearly distributed sources <5.6 and >7.5. The question is how can these sources of plasma, presumably neutrals from Io and Europa, become so distributed. In particular, it is hard for SO_2 or S_2 molecules to have survived the high electron densities near Io and travel inwards to where the molecular ions are observed at 5.3 R_J. One possibility that needs to be investigated is that small dust grains from Io slowly spiral inwards and are slowly eroded away, producing SO_2 or S_2 molecules (M. Horanyi, personal communication, 1993). The possibility that Europa could be a source of plasma first arose from examination of Pioneer 10 UV observations [*Wu et al.*, 1978] and Pioneer 10 plasma data [*Intriligator and Miller*,1982]. *Bagenal* [1989] and *Bagenal et al.* [1992] argue that Voyager observations of higher plasma temperatures and enhanced oxygen composition support a Europa source. Recently, *Schreier et al.'s* [1993] theoretical models suggest that the Europa source is probably less than the Io source by a factor of 10 but could produce significant changes in composition and temperature.

The development of a model of the torus is hampered by not knowing the parallel temperature of the species. The measurements from plasma instrument of Galileo will be particularly important in this regard because of its capability of measuring three-dimensional ion distributions. In the meantime, it would be interesting to quantitatively compare the torus model with the vertical distributions of emissions from various ion species. The Galileo plasma instrument will also be able to distinguish the mass/charge ratios of suprathermal ions, measuring ion fluxes up to 50 keV [*Frank et al.*,

1992]. It will be important to determine the source of these suprathermal ions (whether purely local pick up or other acceleration mechanisms) and to model how the distributions evolve due to collisions or wave-particle interactions.

The model presented in this paper is a starting point for developing more complex models that include longitudinal and local time variations as well as being a reference for monitoring temporal variability of the torus. Perhaps the most critical issue for understanding the Io plasma torus is the nature of radial transport of plasma. Until we can describe the radial transport process(es), it is difficult to give quantitative interpretations of radial profiles of plasma properties or develop quantitative models of the torus chemistry. Ultimately, we need a proper model of the chemistry of the torus which includes (1) an adequate number of species (probably 10 or so); (2) impact ionization, charge-exchange, and recombination reactions; (3) a full description of radiative processes with accurate atomic data; (4) nonthermal distributions for the ions; (5) spatial variations in at least two dimensions; (6) distributed sources of plasma; (7) inward diffusion of hot ions from the plasma sheet; and (8) acceleration of outwardly diffusing material. The homogeneous models of the chemistry and radiation from the torus published by *Barbosa et al.* [1983], *Smith and Strobel* [1985] and *Shemansky* [1988] are important steps in this direction.

Acknowledgments. The author would like to thank Don Shemansky, Ralph McNutt, John Richardson, Arkee Eviatar and Ed Sittler for helpful discussions over the several years taken to put this model together. She acknowledges support for this work by NASA grants NAGW 1622 and 2684 and a JPL contract under the Galileo project.

The Editor thanks E.C. Sittler and another referee for their assistance in evaluating this paper.

References

Angerami, J.J., and J.O. Thomas, Studies of planetary atmospheres, *J. Geophys. Res., 69,* 4537, 1964.

Bagenal, F., J.D. Sullivan and G.L. Siscoe, Spatial distribution of plasma in the Io torus *Geophys. Res. Lett., 7,* 41, 1980.

Bagenal, F., and J.D. Sullivan, Direct plasma measurements in the Io torus and tnner magnetosphere of Jupiter, *J. Geophys. Res., 86,* 8447, 1981.

Bagenal, F., R.L. McNutt, Jr., J.W. Belcher, H.S. Bridge, and J.D. Sullivian, Revised ion temperatures for Voyager plasma measurements in the Io plasma torus, *J. Geophys. Res., 90,* 1755, 1985.

Bagenal, F., Plasma conditions inside Io's orbit: Voyager measurements, *J. Geophys. Res., 90,* 311, 1985.

Bagenal, F., Torus-magnetosphere coupling, Time-variable phenomena in the Jovian system, *NASA Spec. Publ., SP-494,* 196 pp., 1989.

Bagenal, F., D.E. Shemansky, R.L. McNutt, Jr., R. Shreier, and A. Eviatar, The abundance of O^{++} in the Jovian magnetosphere, *Geophys. Res. Lett., 19,* 79, 1992.

Barbosa, D.D., F.V. Coroniti, and A. Eviatar, Coulomb thermal properties and stability of the Io plasma torus, *Astrophys. J., 274,* 429-442, 1983.

Belcher, J. W., The low-energy plasma in the Jovian magnetosphere, in *Physics of the Jovian Magnetosphere,* pp. 68-105, *Cambridge University Press, New York,*1983.

Book, D.L., *NRL Plasma Formulary,* Office of Naval Research, Washington, D.C., 1986.

Bridge, H.S., J.W., Belcher, R.J., Butler, A.J., Lazarus, A.M., Mavretic, J.D., Sullivan, G.L., Siscoe, and V.M. Vasyliunas, The plasma experiment on the 1977 Voyager mission, *Space Sci. Rev., 21,* 259-287, 1977.

Bridge, H.S., et al., Plasma observations near Jupiter: Initial results from Voyager 1 encounter with Jupiter. *Science, 204,* 972-6, 1979.

Broadfoot, A.L., et al., Extreme ultraviolet observations from Voyager 1 encounter with Jupiter. *Science, 204,* 979-982, 1979.

Connerney, J.E.P., Doing more with Jupiter's magnetic field, in *Planetary Radio Emissions III,* Austrian Academy of Sciences Press, Vienna, 1992.

Connerney, J.E.P., M.H. Acuna and N.F. Ness, Voyager 1 assessment of Jupiter's planetary magnetic field, *J. Geophys. Res., 86,* 3623-3627, 1982.

Dessler, A.J., and B.R. Sandel, System III variations in apparent distance of Io plasma torus from Jupiter, *Geophys. Res. Lett., 19,* 2099-2103, 1992.

Divine, N., and H.B. Garrett, Charged particle distributions in Jupiter's magnetosphere, *J. Geophys. Res., 88,* 6889-6903, 1983.

Frank, L.A., K.L. Ackerson, J.A. Lee, M.R. English, and G.L. Pickett, The plasma instrumentation for the Galileo mission, *Space Sci. Rev., 60,* 283-307, 1992.

Intriligator, D.S., and W.D. Miller, First evidence for a Europa plasma torus, *J. Geophys. Res., 87,* 8081, 1982.

Kupo, I., Mekler, Y., and A. Eviatar, Detection of ionized sulfur in the Jovian magnetosphere. *Astrophys. J. Lett., 205,* L51-53, 1976.

Linker, J.A., M.G. Kivelson, M.Moreno, and R.J. Walker, Explanation of the inward displacement of Io's hot plasma torus and consequences for sputtering sources, *Nature, 315,* 375, 1985.

McGrath, M.A., P.D. Feldman, D.F. Strobel, H.W. Moos, G.E. Ballester, Detection of [OII] λ 2471 from the Io plasma torus, *Astrophys. J., 451,* L55, 1993.

McNutt, R.L., J.W. Belcher, and HS. Bridge, Positive ion observations in the middle magnetosphere of Jupiter, *J. Geophys. Res., 86,* 8319, 1981.

Moos, H.W., T.E. Skinner, S.T. Durrance, P.D. Feldman, M.C. Festou, and J.-L. Bertaux, Long term stability of the high-temperature plasma torus, *Astrophys. J., 294,* 369-382, 1985.

Moos, H.W., et al., Determination of ionic abundances in the Io torus using the Hopkins Ultraviolet Telescope, *Astrophys. J., 382,* L105, 1991.

Morgan, J.S., Temporal and spatial variations in the Io torus, *Icarus, 62,* 389, 1985.

Richardson, J.D., and G.L. Siscoe, Factors governing the ratio of inward to outward diffusing flux of satellite ions, *J. Geophys. Res., 86,* 8485-8490, 1981.

Schreier, R., A. Eviatar, V.M.Vasyliunas, J.D. Richardson, Modeling the Europa plasma torus, *J. Geophys. Res., 98,* 21,231-21,243, 1993.

Shemansky, D.E., Energy branching in the Io plasma torus: The failure of neutral cloud theory, *J. Geophys. Res., 93,* 1773, 1988.

Siscoe, G.L., On the equatorial confinement and velocity space distribution of satellite ions in Jupiter's magnetosphere, *J. Geophys. Res., 82,* 1641, 1977.

Siscoe, G.L., Jovian plasmaspheres, *J. Geophys. Res., 83,* 2118-2126, 1978.

Siscoe, G.L., A. Eviatar, R.M. Thorne, J.D. Richardson, F.

Bagenal, and J.D. Sullivan, Ring current impoundment of the Io plasma torus, *J. Geophys. Res., 86,* 8480, 1981.

Sittler, E.C., and D.F. Strobel, Io plasma torus electrons: Voyager 1, *J. Geophys. Res., 92,* 5741, 1987.

Smith, R.A., and D.F. Strobel, Energy partitioning in the Io plasma torus, *J. Geophys. Res., 90,* 9469, 1985.

Stone, R.G., et al., Ulysses radio and plasma wave observations in the Jupiter environment, *Science, 257,* 1524, 1992.

Thomas, N., Detection of [O III] λ5007 emission from the Io plasma torus, *Astrophys. J., 414,* L41, 1993.

Tokar, R.L., D.A. Gurnett and F.Bagenal, The proton concentration in the vicinity of the Io plasma torus, *J. Geophys. Res., 87,* 10,395-10,400, 1982.

Warwick, J.W., et al., Voyager 1 Planetary Radio Astronomy observations near Jupiter, *Science, 204,* 995-998, 1979.

Wu, F.-M., D.L. Judge, and R.W. Carlson, Europa: Ultraviolet emissions and the possibility of atomic oxygen and hydrogen clouds, *Astrophys. J., 225,* 325, 1978.

F. Bagenal, Astrophysical, Planetary and Atmospheric Sciences Dept., Campus Box 391, University of Colorado, Boulder, CO 80309-0391.

(Received July 12, 1993; revised October 6, 1993; accepted October 11, 1993.)